Aliovalent cation ordering, coexisting ferroelectric structures, and electric field induced phase transformation in lead-free ferroelectric $Na_{0.5}Bi_{0.5}TiO_3$

Jaysree Pan, Manish K. Niranjan, and Umesh V. Waghmare

Citation: J. Appl. Phys. **119**, 124102 (2016); doi: 10.1063/1.4944473
View online: http://dx.doi.org/10.1063/1.4944473
View Table of Contents: http://aip.scitation.org/toc/jap/119/12
Published by the American Institute of Physics

Aliovalent cation ordering, coexisting ferroelectric structures, and electric field induced phase transformation in lead-free ferroelectric $Na_{0.5}Bi_{0.5}TiO_3$

Jaysree Pan,[1] Manish K. Niranjan,[2] and Umesh V. Waghmare[1]
[1]*Theoretical Sciences Unit, Sheikh Saqr Laboratory, Jawaharlal Nehru Centre for Advance Scientific Research, Jakkur, Bangalore 560064, India*
[2]*Department of Physics, Indian Institute of Technology, Hyderabad, 502285, India*

(Received 20 November 2015; accepted 1 March 2016; published online 22 March 2016)

Using first-principles calculations, we show that a specific chemical ordering of Na and Bi in $Na_{0.5}Bi_{0.5}TiO_3$ is responsible for the co-existence of its ferroelectric phases with rhombohedral *R3c* and monoclinic *Cc* structures, which are relevant to its morphotropic phase boundary and large piezoelectric response. We identify the signatures of chemical ordering in the calculated phonon spectra and establish the prevalence of A-type ordering through comparison with experiment. We uncover a mechanism of the observed electric field induced *Cc* to lower energy *R3c* structural transformation promoted by a hybrid soft mode involving a combination of TiO_6 rotations and a polar component. © *2016 AIP Publishing LLC*.
[http://dx.doi.org/10.1063/1.4944473]

I. INTRODUCTION

$Na_{0.5}Bi_{0.5}TiO_3$ (NBT) is an important material with a large piezoelectric response[1–8] and has the potential for replacement of lead based ferroelectric ceramics such as lead zirconate titanate (PZT) used extensively in commercial piezoelectric actuators devices. It is also the base material for newly discovered family of oxide ion conductors with promising application in solid oxide based fuel cell.[9] NBT has a distorted perovskite ABO_3 structure, with mixed site occupancy of Na^{1+} and Bi^{3+} ions at *A*-site, and Ti^{4+} at the octahedrally coordinated B-site. The former results in aliovalent partial order or disorder of cations at *A*-site that is relevant to its relaxor ferroelectric properties.[6,10] Substitution of K and Na at *A* site,[7] for example, has been shown to result in local structural disorder. The ferroelectric phase of NBT readily transforms to its antiferroelectric,[2] non-polar,[4,5] or other ferroelectric phases[5,11,12] with applied electric field or as a function of temperature, which is responsible for its large strain response properties.[4] The stability of these phases depends sensitively on the local chemical composition and the way in which Na and Bi are chemically ordered.[2,6,7] The relationship between the chemical ordering and structure is fundamental to its properties. For example, a giant piezoelectric response (of PZT, for example) is typically attributed to morphotropic phase boundary (MPB) in lead based ferroelectrics, or to nano-scale structural heterogeneities known as nano-polar regions (NPRs) in relaxors, in which they correlate with nano-scale chemically ordered regions.[13] NBT has been shown recently to exhibit coexistence of rhombohedral *R3c* and monoclinic *Cc* structures at room temperature,[11,12] both of which are ferroelectric. To be able to introduce an MPB in lead-free ferroelectrics such as NBT, it is important to understand the relative stability of its *R3c* and *Cc* phases and its dependence on ordering of Na and Bi.

NBT is also known to undergo a *Cc* to *R3c* phase transition upon application of electric field, depending on its mechanical or thermal treatment.[11,12,14] In the *R3c* structure, polarization is along [111] direction, while it is in the (110) plane of the *Cc* structure, which arises from off-centering of Ti and Bi cations with respect to O anions.[10] The existence of *Cc* structure in the form of local structural heterogeneities or nano-regions makes the untreated NBT a relaxor with short range polar order.[13] After elimination of such polar nano-regions by forcing a *Cc* to *R3c* phase transition, NBT becomes a normal ferroelectric,[12] with *R3c* structure and polarization of $\approx 38\ \mu C/cm^2$.[10]

The *R3c* and *Cc* structures of NBT differ from each other primarily in terms of tilting of TiO_6 octahedra. In the *R3c* structure, TiO_6 octahedral tilting has $a^-a^-a^-$ ordering, while it orders in $a^-a^-c^-$ manner in the *Cc* structure. Observation of small in-phase tilting in the untreated NBT constituted of *R3c* and *Cc* structures can be argued as manifestation of orientation mismatch between the two antiphase tilts of $a^-a^-a^-$ and $a^-a^-c^-$ at their domain boundaries.[15] In studies of defects and their symmetry in single-crystalline NBT, high energy antiphase boundaries were observed. Their incompatibility with antiphase tilting of the oxygen octahedra in *R3c* matrix forms high density of nano-twins that have the width of a few unit cells, and ions there locally adopt a variable *Cc* symmetry with $a^-a^-c^-$ tilting.[16] The Cc structure of NBT is considered to be metastable because of the irreversibility of *Cc* to *R3c* phase transition.[11,12] Properties of the perovskite structure are quite sensitive to BO_6 octahedral tilts, which influence its electronic, magnetic, and dielectric properties.

Some theoretical works have so far attempted to develop basic understanding of this lead-free ferroelectric material and its structural, electronic, ferroelectric, dielectric properties of pristine NBT,[10,17,18] and effects of *A*-site nonstoichiometry, O-vacancy, and doping on its properties.[19–21] In addition, a few theoretical studies focused on thin films of

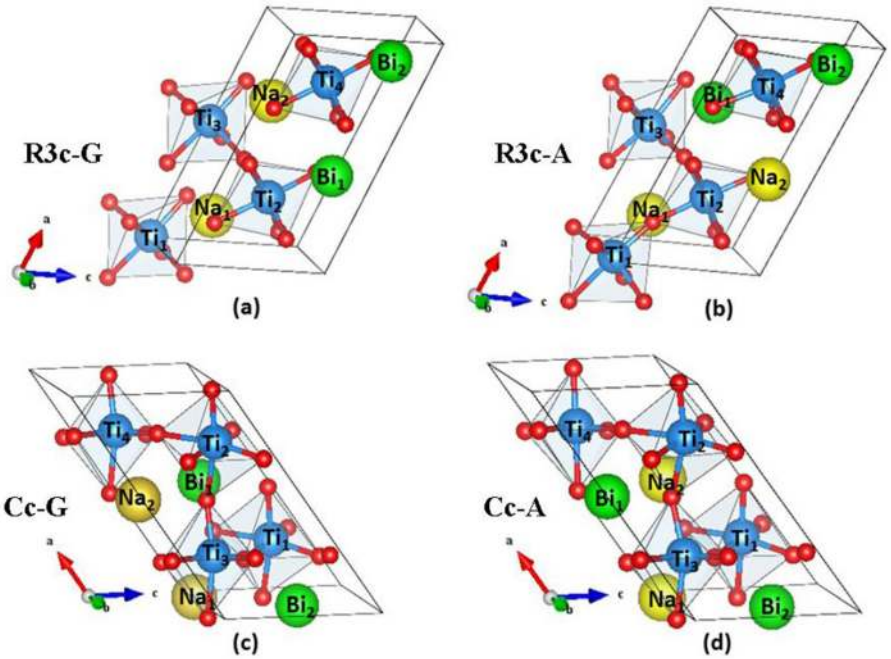

FIG. 1. Crystal structures of (a) *R3c-G*, (b) *R3c-A*, (c) *Cc-G*, and (d) *Cc-A* phases of NBT after relaxation. Red balls are O atoms.

NBT and its surface.[22,23] While earlier calculations focused on temperature induced phase transformation of NBT (cubic to tetragonal to rhombohedral phase transition), the recent observation[11,12] of the co-existence of two ferroelectric phases (*R3c* and *Cc*) of NBT is key to relaxor properties and needs to be understood. In this article, we investigate ordering of Na and Bi ions at *A*-sites, and its influence on the relative stability and coexistence of *R3c* and *Cc* phases. We then determine a possible soft-mode based mechanism of electric field driven *Cc* to *R3c* structural transformation in NBT.

Our analysis is based on first-principles density functional theory (DFT)[24] based calculations. We use Quantum Espresso[25] implementation of DFT with ultra-soft pseudopotentials to model interaction between ionic cores and valence electrons[25,26] and a local density approximation (LDA) of the exchange-correlation energy functional. NBT is a good non-magnetic insulator with relaxor ferroelectric properties, and our simulations do not include any spin dependent density or properties. We use a kinetic energy cutoff of 30 Ry in truncation of the basis set to represent wave functions, and a cutoff of 240 Ry for representing density. Brillouin zone integrations are sampled with uniform $3 \times 6 \times 6$ k-mesh for each NBT phase. Born-effective charge tensor and zone center phonon frequencies have been obtained employing density functional perturbation theory (DFPT) as implemented in Quantum Espresso package.

II. RESULTS AND DISCUSSION

To determine the effects of chemical ordering of Na^{1+} and Bi^{3+} in NBT, we have considered *G* and *A* type ordering in both *R3c* (Figs. 1(a) and 1(b)) and *Cc* (Figs. 1(c) and 1(d)) structures. Each of these states of chemical ordering can be modelled with a periodic super-cell containing two Na (Na_1 and Na_2), two Bi (Bi_1 and Bi_2), four Ti (Ti_1, Ti_2, Ti_3 and Ti_4), and twelve O atoms (see supplementary Table I[37]). In the G-type ordering, the nearest neighbor A-sites of each Na atom are all occupied by Bi atoms (and vice versa). On the other hand, two of the nearest neighbors A-sites of each Na atom are occupied by Na atoms and rest of the nearest neighbor A-sites by Bi atoms in *A*-type ordering. We find that the lattice parameters of *R3c* and *Cc* structures do not change much with variation in the *A*-site cationic ordering (G/A type), as our estimates of lattice parameters of each of these structures (see Table I) are in good agreement with their experimental values.[11,12,14] However, the ordering at *A*-site does impact the stability of the structure. For any of the *R3c* and *Cc* structures, *A*-type ordering has a significantly lower energy than the *G*-type ordering (see Table II). Clearly, *R3c*

TABLE I. Theoretically optimized structural details of both *R3c* and *Cc* phases of NBT supercell (i.e., $Na_2Bi_2(TiO_3)_4$). The lattice parameter values inside the brackets are taken from experiments.[8–10]

	Lattice parameter (supercell)						
Phase	a (Å)	b (Å)	c (Å)	α (°)	β (°)	γ (°)	Volume (Å^3)
R3c-G	10.84 (10.98)	5.42 (5.49)	5.42 (5.49)	59.5 (59.8)	59.5 (59.8)	59.5 (59.8)	222.8
R3c-A	10.85 (10.98)	5.43 (5.49)	5.43 (5.49)	59.2 (59.8)	59.5 (59.8)	59.7 (59.8)	223.2
Cc-A	9.32 (9.52)	5.40 (5.48)	5.44 (5.51)	90.0 (90.0)	125.2 (125.3)	90.0 (90.0)	223.6
Cc-G	9.32 (9.52)	5.38 (5.48)	5.42 (5.51)	90.0 (90.0)	125.0 (125.3)	90.0 (90.0)	222.8

TABLE II. Relative energy ($\Delta E_{relative}$) per formula unit ($Na_{0.5}Bi_{0.5}TiO_3$), electronic band gap (Δ_{gap}), Berry phase polarization (P) of *R3c* and *Cc* phases of NBT.

Phase	$\Delta E_{relative}$ (eV)	Δ_{gap} (eV)	P ($\mu C/cm^2$)
R3c-G	41.5	2.52	26.3
R3c-A	00.0	2.39	37.4
Cc-A	19.0	2.40	29.9
Cc-G	41.5	2.44	28.3

structure with *A*-type ordering (*R3c-A*) has the lowest energy among the four configurations considered here.

Cc structure with *A*-type ordering (*Cc-A*) is ≈19 meV/f.u. higher in energy than *R3c* structure with A-type ordering (*R3c-A)*. On the other hand, both *R3c* and *Cc* structures with *G*-type ordering (*R3c-G* and *Cc-G*) are much higher in energy (by ≈41 meV/f.u higher than *R3c-A*). Clearly, *A*-type ordering is favored at low temperatures in well-annealed sample of NBT. The fact that *Cc-A* is energetically close to *R3c-A* points at a possible co-existence of these structures in NBT. Stability of a slightly higher energy *Cc-A* structure in real samples may be further increased by strains associated with local structural disorder, for example, twin boundaries, in the global *R3c* matrix of NBT.[12,14]

The symmetry of NBT is lowered by (a) chemical ordering as well as (b) structural distortions with respective to higher symmetry cubic perovskite structure, both of which are reflected in its electronic structure (see electronic density of states in Fig. 2). We will show that *R3c-A* has the lowest symmetry due to its *A*-type chemical ordering over *G*-type ordering in *A*-site ions in NBT, which correlates with its lowest energy. From the total and projected density of states (pDoS, projected on valence atomic orbitals) of NBT (Fig. 2), we note that the valence band, of about 5.8 eV bandwidth, is mainly constituted of *O-2p* bands. A band-gap of about 2.2 eV separates the *O-2p* valence band from the lowest energy *Ti-3d* conduction band, and our estimate of the band gap of *R3c-G* structure is in good agreement with estimates of earlier calculations on the same structure.[16,17] About 3 eV below the valence band, there is a small subband primarily made of 6s orbitals of Bi. *3s* orbitals of Na and *6p* orbitals of Bi contribute to both valence and conduction bands, at very similar energies reflecting on the covalency of Na-O and Bi-O bonds, and compatibility of Na^{1+} and Bi^{3+} to be at *A*-site.

To assess the symmetry of various sites, we now closely examine the pDoS. The inequivalence between contributions of *2p* orbitals of different oxygen atoms to the valence band in states with *A*-type ordering is clearly reflected in several peaks and distinct curve for each atom in the pDoS. In contrast, there are only two inequivalent sets of pDoS in the state with *G*-type ordering. The conduction bands of all the four configurations confirm the octahedral splitting of *3d* states of Ti, with lower energy peak of t_{2g} and higher energy peak of e_g states. Relatively lower site symmetry of Ti in A-type ordering results in further splitting of these peaks in the *A*-type ordering, and the gap between peaks of t_{2g} and e_g bands essentially disappears. In contrast, this gap remains intact in the two configurations with *G*-type ordering. We suggest that this constitutes an observable electronic spectral signature of the type of ordering at *A*-sites of NBT. The lowest symmetry of *R3c-A* among the four configurations considered here is clearly evident also in the contribution of *3d* orbitals of its Ti atoms to pDoS, which exhibits many peaks (Fig. 2) associated with the split bands.

The lone pair electrons of Bi (6s-orbital) are known to cause off-centering of Bi atoms and drives ferroelectricity of Bi-based oxides.[21] The peak associated with *Bi-6s* states in the pDoS of *G*-type ordered NBT is notably sharper than that in the *A*-type ordered NBT (Fig. 2). The sharper peak of *Bi-6s* states indicates that the lone pair electrons of Bi have less deviation from the high symmetry spherical shape of s-orbital. This means a weaker interaction between the Bi-6s lone pair electrons with its neighboring electronegative O-ions in the *G*-type ordered NBT than in the *A*-type ordered NBT. The disparity in lone pair electrons of Bi and its influence on the intrinsic polarization of NBT are obvious in the calculated polarization with Berry phase method (Table II): *A*-type ordered structure has a higher dipole moment than that of the *G*-type ordered structure, consistent with greater delocalization of its lone pair electron of Bi. In A-type ordered NBT, the delocalization of Bi 6s lone pair is more significant in *Cc-A* structure than in *R3c-A* (Fig. 2). However, *R3c-A* exhibits a higher polarization than *Cc-A*. This is because the hybridization of *3d* orbitals of Ti with *2p* orbitals of O also contributes to polarization, and likely to be more significant in the *R3c-A* configuration, consistent with its lower symmetry and estimates of earlier observations.[16,28,29] Our estimate of spontaneous polarization using Berry phase method shows that polarization of *R3c-A* phase is very close to the measured (see Table II) polarization of pure *R3c*.[10]

We now identify signatures of the chemical ordering at A-site in NBT in its vibrational spectrum (see supplementary Table II[37]) by comparing our calculated frequencies of the zone center phonons of the four configurations of NBT (Table III) with experimental Raman and IR spectra. Clearly, a combination of phonon spectra of *R3c-A* and *Cc-A* structures has to be considered to cover all the observed modes (see Table III for all the Raman (R) and infrared (IR) modes reported experimentally[10,30,31]). Specifically, low frequencies modes at 120 (R) and 126 (IR) cm^{-1} and high frequency modes at 860 (R), 869 (R) and 879 (IR) cm^{-1} belong to the spectrum of *A*-type ordering and *not* to that of G-type. This confirms our conclusion based on energies that *A*-type ordering is favored in NBT at room temperature. Secondly, the observed modes at 750, 585, and 142 cm^{-1} can be explained only from the calculated modes of *Cc-A* configuration, and the observed modes at 820 and 875 cm^{-1} are represented in the calculated spectrum of *R3c-A* only, among the configurations with *A*-type ordering. Consistent with relatively lower symmetry of A-type ordering, *R3c-A* shows the hardest frequency mode while *Cc-A* exhibits the softest of the modes of all four structures (see Fig. 3).

A Born effective charge tensor gives the coupling of electric field with atomic displacements, i.e., phonons. They often deviate anomalously from the nominal ionic charges of atoms in perovskite ferroelectric oxides and are good

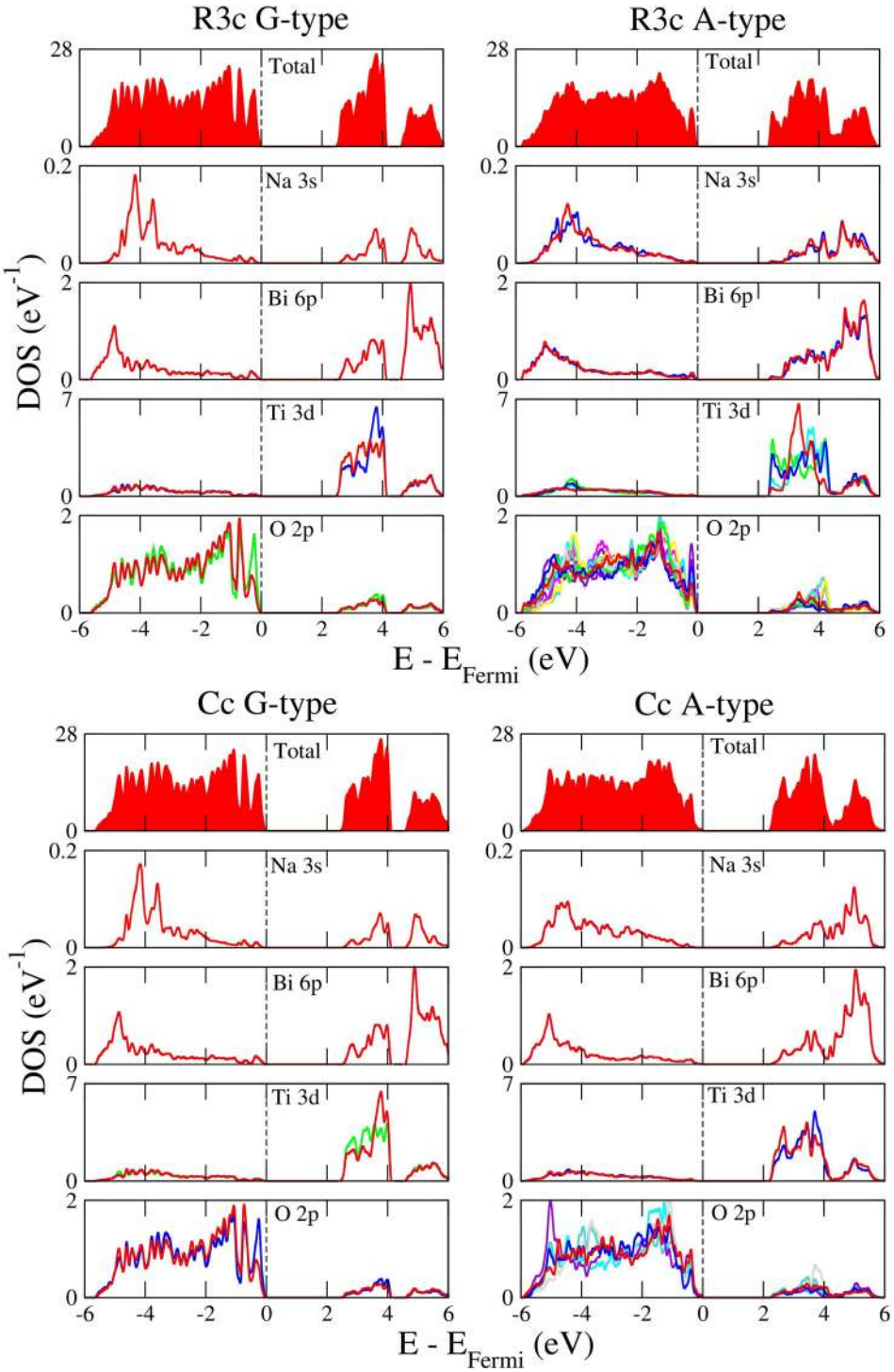

FIG. 2. Total and projected electronic density of states of the *A*- and *G*-type ordered *R3c* and *Cc* phases of NBT. Different color lines are used to indicate the orbitals of different ions. For Bi ions, green and red colors represent 6s and 6p orbitals.

indicators of a material to undergo ferroelectric transition.[27,32,33] Relatively lower symmetry of a structure with *A*-type ordering compared to that with *G*-type ordering in NBT is nicely reflected in grouping of atoms based on their Born effective charge tensors (see supplementary Table III[37]). In *G*-type ordering, effective charge tensors are mostly diagonal, with small antisymmetric off-diagonal component on Bi and Ti ions. Born effective charge tensors of atoms in the A-type structure exhibit lower symmetry: they are anisotropic for each of Na, Bi, and Ti ions, pointing out the lower symmetry in *A*-type ordering. This anisotropy is even more prominent in *R3c-A* than in *Cc-A* confirming our conclusion of its lower symmetry in terms of electronic structure. For example, Born charges of Ti in the *R3c-A* structure exhibit notable off-diagonal components, some of which are as high as 1.57. Secondly, the range of effective charges of Ti is wider in configurations of *A*-type ordering. A strong deviation of Born charges of Bi from its nominal 3+ state is well-known.[12,14] It reflects important role played by Bi in ferroelectricity through off-centering. Our results reveal that the deviation of Born charge of Bi from 3+ is less in the *A*-type ordering than that in the *G*-type ordering, consistent with delocalization of its lone pair *6s* states. The most important aspect of the Born charges estimates here is the remarkable

TABLE III. Gamma point frequencies (cm^{-1}) of *R3c* and *Cc* phase of NBT. Experimental frequencies are from Raman and IR studies at room temperature.

Theory				
R3c-G	*R3c-A*	*Cc-A*	*Cc-G*	Experiment[8,22,23]
…	121	123, 125	…	120 (R), 126 (IR)
133	133, 135	…	132	131 (R)
147	…	143	…	141 (R), 142 (R)
158, 160, 164	158, 168	158, 162	159, 160, 167	158 (IR), 165 (R)
221,223	221, 227	216, 229	229	220 (R), 227 (IR)
234	239	231	235	235 (R)
276, 278	278	276, 288, 289	278, 289	274 (R), 279 (R), 281 (R), 287 (IR)
303, 305	303, 304	306	303, 317	306 (R)
337, 345	340, 344	337	339, 346	340 (R)
350	356	354	352, 356	351 (IR)
403, 410, 411	405, 412	401, 414	402, 409, 411	406 (IR)
…	503	504	499	490 (R), 491 (R)
…	519	511, 514	513	515 (IR)
542	539	532	531	521 (R), 527 (R), 531 (R)
554	545	553	560	551 (IR)
575	569	567	575	573 (R), 576 (R)
580, 593	…	593	593	585 (R)
…	645	621	615	634 (IR)
…	…	762	764	748 (R), 750 (R), 754 (R)
785	772	…	…	775 (IR)
…	…	814	802	803 (R)
818, 823	821	…	828	820 (R), 823 (IR), 829 (R)
…	877	…	…	860 (R), 869 (R), 875 (IR)

disparity in the charges of Na (∼1.11) and Bi (5.1), both of which occupy A-site. This subsequently results in differences in the Born charges of different Ti ions on the lattice, due to charge neutrality.

It is well-known that relaxor behavior arises from NPRs, which correlate with short-range chemical (cationic) ordering.[13] Indeed, such regions do not form in solid solutions in which cations have the same nominal charge, like lead zirconate-titanate. On the other hand, the classic relaxors, $PbMg_{1/3}Nb_{2/3}O_3$ and $PbSc_{1/2}Nb_{1/2}O_3$, exhibit NPRs that relate to ordering of hetero-valent Mg and Nb (or Sc and Nb) cations at *B* sites. Since the local dipole moment or polarization is given by the Born charges, the disparity in Born charges of the cations at *A* or *B* sites in perovskites is an accurate measure of hetero-valency, and expected to be a good descriptor of a material's tendency to exhibit NPRs and hence the relaxor behavior. In NBT, ordering or weak disorder in occupancy such as aliovalent, hetero-polar substitutional ions are thus central to possible NPRs and their relaxor ferroelectric properties, and diffuse ferroelectric transitions. Indeed, we expect the ordering (*A*-type) along with substitutional disorder (deviations to *G*-type) at *A*-site in NBT to be key to its relaxor properties. We find that average static dielectric response of *R3c-G* structure (see supplementary Table IV[37]) is the largest (∼100) among the four configurations, while that of *R3c-A* structure is about 86. Average dielectric response of *Cc-A* and *Cc-G* configurations is about the same (79 and 81, respectively).

Based on our results for phonons, we now propose a soft-mode based mechanism for the structural transformation

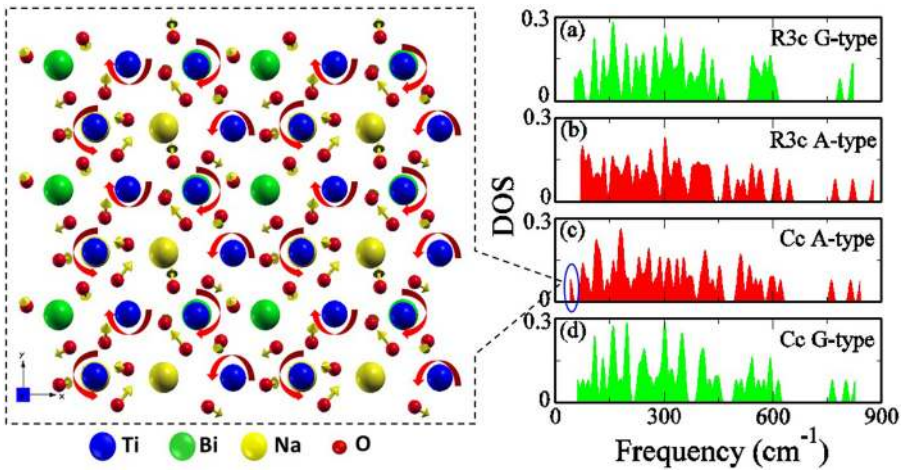

FIG. 3. Right plot is the comparison between phonon frequencies of (a) *R3c-G*, (b) *R3c-A*, (c) *Cc-A*, and (d) *Cc-G* phases of NBT (For details, please see the supplementary Table II).[37] The blue elliptical enclosure is showing the softest mode in the *Cc-A* (c) phase. The right side plot is the visualization of softest phonon mode (∼40 cm^{-1}) found in the *Cc-A* (Yellow arrows are showing the Eigen vector on each atom, and red colored curved arrows are schematically representing the rotation motion of oxygen octahedra following the eigen vector direction around Ti atoms).

of *R3c* to *Cc* structure (with the same ordering of Na^{1+} and Bi^{3+}). The *R3c* and *Cc* structures essentially differ in their TiO_6 octahedral tilts with respect to the reference cubic perovskite structure. *R3c* structure has a similar antisymmetric tilt around each of its crystal axis ($a^-a^-a^-$), while *Cc* structure involves the same antisymmetric tilt around a- and b-axis, but a different one around c axis, ($a^-a^-c^-$). Hence, *Cc* to *R3c* phase transformation by the application of external perturbation such as electric filed necessarily involves rotations of TiO_6 octahedra in the *Cc* structure around c-axis to reorganize themselves in $a^-a^-a^-$ manner, and to give *R3c* structure. From a careful examination of eigenvectors of various low energy phonons, we find a clue to the electric field driven *Cc* to *R3c* phase transformation in the softest phonon mode at $\approx 40\,cm^{-1}$ of *Cc-A* structure (see Fig. 3), which is hybrid in character. While its eigen vector involves mainly the displacements of O ions to give TiO_6 octahedral rotations (Fig. 3), it does have a nonzero electric dipole moment associated with Bi displacements making it a polar mode that couples with electric field. Displacements of O ions in this mode represent antisymmetric rotational motif (marked by red arrows in Fig. 3), whose axis is slanted with respect to z-direction. This is expected as c-axis of *Cc* phase is itself tilted from z-axis by $\approx 35°$. Due to its polar nature and low frequency, this mode responds rather strongly to applied field and generates rotations of TiO_6 octahedra and tilts, leading to transformation of *Cc-A* structure to *R3c-A* structure. This gives a possible mechanism of the observed transition of NBT from relaxor state to a ferroelectric one with applied electric field. In literature,[34–36] the observed lowest frequencies of Raman or IR modes of NBT are in the range from 45 to $55\,cm^{-1}$ at low temperatures ($\sim 10\,K$). Hence, soft modes do exist in NBT, and it was also found in these works that these soft Raman/IR modes are quite sensitive to temperature and become even softer with increasing temperature. However, the specific phase of NBT (pure *R3c* or mixed phase of *R3c* and *Cc*) is hard to be determined experimentally alone, and predictions in our work will be useful in the interpretation of Raman or IR spectra, the future experiments.

III. CONCLUSION

We have presented a quantitative analysis of the stability of chemical ordering of cations at A-site in NBT and associated ferroelectric structures with *R3c* and *Cc* space groups. From the energetics, we conclude that *A*-type ordering of Na and Bi is prevalent in experimental samples of NBT, and that the metastable *Cc* phase is expected to coexist in the matrix of largely *R3c* phase. Comparing our calculated frequencies of Raman and IR active phonons of NBT with experimental vibrational spectra, we confirm that chemical ordering of Na and Bi is largely of *A*-type, and conclude that the co-existence of *R3c* and *Cc* is necessary to explain all the observed modes, as concluded in the recent experimental work. We provide electronic spectral signatures of the *A*-type ordering (as opposed to *G*-type) in NBT, which will facilitate further verification from the experiment. We show large differences in Born charges of different Ti atoms (and of Na, Bi), which are the descriptors of relaxor behavior of NBT. Finally, we have provided a possible mechanism based on a hybrid soft-mode that provides a path of electric field driven transition from *Cc* to *R3c* structure in NBT, which is key to large strain piezoelectric response of NBT.

ACKNOWLEDGMENTS

U.V.W. acknowledges support from a JC Bose National Fellowship of the Department of Science and Technology, Government of India.

[1]Y. M. Chiang, G. W. Farrey, and A. N. Soukhojak, Appl. Phys. Lett. **73**, 3683 (1998).
[2]Y. Guo, M. Gu, H. Luo, Y. Liu, and R. L. Withers, Phys. Rev. B **83**, 054118 (2011).
[3]Y. Hiruma, H. Nagata, and T. Takenaka, J. Appl. Phys. **105**, 084112 (2009).
[4]W. Jo, T. Granzow, E. Aulbach, J. Rödel, and D. Damjanovic, J. Appl. Phys. **105**, 094102 (2009).
[5]J. E. Daniels, W. Jo, J. Roedel, and J. L. Jones, Appl. Phys. Lett. **95**, 032904 (2009).
[6]J. Kreisel, P. Bouvier, B. Dkhil, P. A. Thomas, A. M. Glazer, T. R. Welberry, B. Chaabane, and M. Mezouar, Phys. Rev. B **68**, 014113 (2003).
[7]V. A. Shuvaeva, D. Zekria, A. M. Glazer, Q. Jiang, S. M. Weber, P. Bhattacharya, and P. A. Thomas, Phys. Rev. B **71**, 174114 (2005).
[8]X. Liu and X. Tan, Adv. Mater. **28**, 574 (2016).
[9]M. Li, M. J. Pietrowski, R. A. De Souza, H. Zhang, I. M. Reaney, S. N. Cook, J. A. Kilner, and D. C. Sinclair, Nat. Mater. **13**, 31 (2014).
[10]M. K. Niranjan, T. Karthik, S. Asthana, J. Pan, and U. V. Waghmare, J. Appl. Phys. **113**, 194106 (2013).
[11]B. N. Rao, A. N. Fitch, and R. Ranjan, Phys. Rev. B **87**, 060102 (2013).
[12]B. N. Rao, R. Datta, S. S. Chandrashekaran, D. K. Mishra, V. Sathe, A. Senyshyn, and R. Ranjan, Phys. Rev. B **88**, 224103 (2013).
[13]S. Tinte, B. P. Burton, E. Cockayne, and U. V. Waghmare, Phys. Rev. Lett. **97**, 137601 (2006).
[14]B. N. Rao and R. Ranjan, Phys. Rev. B **86**, 134103 (2012).
[15]R. Beanland, Acta Cryst. A **67**, 191 (2011).
[16]R. Beanland and P. A. Thomas, Phys. Rev. B **89**, 174102 (2014).
[17]H. Lü, S. Wang, and X. Wang, J. Appl. Phys. **115**, 124107 (2014).
[18]R. Bujakiewicz-Korońska and Y. Natanzon, Phase Transitions **81**, 1117 (2008).
[19]L. Ju, C. Shi, L. Sun, Y. Zhang, H. Qin, and J. Hu, J. Appl. Phys. **116**, 083909 (2014).
[20]J. A. Dawson, H. Chen, and I. Tanaka, J. Mater. Chem. A **3**, 16574 (2015).
[21]X. He and Y. Mo, Phys. Chem. Chem. Phys. **17**, 18035 (2015).
[22]M. Bousquet, J.-R. Duclère, E. Orhan, A. Boulle, C. Bachelet, and C. Champeaux, J. Appl. Phys. **107**, 104107 (2010).
[23]P. Petrov, H. Guhl, and W. Miller, Phys. Status Solidi B **245**, 2649 (2008).
[24]W. Kohn and L. J. Sham, Phys. Rev. **140**, A1133 (1965).
[25]D. Vanderbilt, Phys. Rev. B **41**, 7892 (1990).
[26]P. Giannozzi, S. Baroni, N. Bonini, M. Calandra, R. Car, C. Cavazzoni, D. Ceresoli, G. L. Chiarotti, M. Cococcioni, I. Dabo, A. Dal Corso, S. de Gironcoli, S. Fabris, G. Fratesi, R. Gebauer, U. Gerstmann, C. Gougoussis, A. Kokalj, M. Lazzeri, L. Martin-Samos, N. Marzari, F. Mauri, R. Mazzarello, S. Paolini, A. Pasquarello, L. Paulatto, C. Sbraccia, S. Scandolo, G. Sclauzero, A. P. Seitsonen, A. Smogunov, P. Umari, and R. M. Wentzcovitch, J. Phys.: Condens. Matter **21**, 395502 (2009).
[27]P. Baettig, C. F. Schelle, R. LeSar, U. V. Waghmare, and N. A. Spaldin, Chem. Mater. **17**, 1376 (2005).
[28]D. S. Keeble, E. R. Barney, D. A. Keen, M. G. Tucker, J. Kreisel, and P. A. Thomas, Adv. Funct. Mater. **23**, 185 (2013).
[29]E. Aksel, J. S. Forrester, J. L. Jones, P. A. Thomas, K. Page, and M. R. Suchomel, Appl. Phys. Lett. **98**, 152901 (2011).
[30]I. G. Siny, E. Husson, J. M. Beny, S. G. Lushnikov, E. A. Rogacheva, and P. P. Syrnikov, Ferroelectrics **248**, 57 (2000).

[31]J. Suchanicz, I. J. Sumara, and T. V. Kruzina, J. Electroceram. **27**, 45 (2011).
[32]W. Zhong, R. D. King-Smith, and D. Vanderbilt, Phys. Rev. Lett. **72**, 3618 (1994).
[33]U. Waghmare, N. Spaldin, H. Kandpal, and R. Seshadri, Phys. Rev. B **67**, 125111 (2003).
[34]S. G. Lushnikov, S. N. Gvasaliya, I. G. Siny, I. L. Sashin, V. H. Schmidt, and Y. Uesu, Solid State Commun. **116**, 41 (2000).
[35]J. Petzelt, S. Kamba, J. Fábry, D. Noujni, V. Porokhonskyy, A. Pashkin, I. Franke, K. Roleder, J. Suchanicz, R. Klein, and G. E. Kuge, J. Phys.: Condens. Matter **16**, 2719 (2004).
[36]I. G. Siny, E. Husson, J. M. Beny, S. G. Lushnikov, E. A. Rogacheva, and P. P. Syrnikov, Phys. B **293**, 382 (2001).
[37]See supplementary material at http://dx.doi.org/10.1063/1.4944473 for atomic positions, zone centred phonon frequencies, Born effective charges and dielectric constants of R3c-G, R3c-A, Cc-A and Cc-G phases.